IOP Conf. Series: Journal of Physics: Conf. Series **797** (2017) 012004 doi:10.1088/1742-6596/797/1/012004

A model to predict the ultrasonic field radiated by magnetostrictive effects induced by EMAT in ferromagnetic parts

B Clausse[1], A Lhémery[1] and H Walaszek[2]
[1] CEA LIST, F-91191, Gif-sur-Yvette, France
[2] CETIM, F-60304, Senlis, France

E-mail: alain.lhemery@cea.fr

Abstract. An Electro-Magnetic Acoustic Transducer (EMAT) is a non-contact source used in Ultrasonic Testing (UT) which generates three types of dynamic excitations into a ferromagnetic part: Lorentz force, magnetisation force, and magnetostrictive effect. This latter excitation is a strain resulting from a magnetoelastic interaction between the external magnetic field and the mechanical part. Here, a tensor model is developed to transform this effect into an equivalent body force. It assumes weak magnetoelastic coupling and a dynamic magnetic field much smaller than the static one. This approach rigorously formulates the longitudinal Joule's magnetostriction, and makes it possible to deal with arbitrary material geometries and EMAT configurations. Transduction processes induced by an EMAT in ferromagnetic media are then modelled as equivalent body forces. But many models developed for efficiently predicting ultrasonic field radiation in solids assume source terms given as surface distributions of stress. To use these models, a mathematical method able to accurately transform these body forces into equivalent surface stresses has been developed. By combining these formalisms, the magnetostrictive strain is transformed into equivalent surface stresses, and the ultrasonic field radiated by magnetostrictive effects induced by an EMAT can be both accurately and efficiently predicted. Numerical examples are given for illustration.

1. Ultrasonic Testing using EMAT in ferromagnetic materials

In Ultrasonic Testing (UT), elastic waves are generated into the solid under examination by transducers. In most cases, piezoelectric transducers are used, operating from outside through a medium which mechanically couples them to the solid. When the use of such coupling is avoided or if piezoelectric transducers are not adapted to the need, the implementation of alternative non-contact solutions is required. For this, the piece under examination is excited by an external source of a physical field of non-mechanical nature (e.g. electromagnetic). The interaction of this field with the elastic part converts the non-mechanical energy involved into dynamic mechanical effects within the piece material, which in turn becomes a source of elastic waves. Electro-Magnetic Acoustic Transducers (EMAT) [1,2] are among the main non-contact probes currently used in UT. Since no coupling medium is needed, such sensors are practically suitable to operate in harsh conditions (high gradients of pressure, temperature). Another attractive aspect of EMAT consists in its ability to excite multiple modes with a high reproducibility, giving the opportunity to design various testing applications [3]. However, EMATs usually present low signal-to-noise ratios (compared to piezoelectric ones), and are strongly configuration and material dependent which brings some complexities to the modelling process. Generally, EMATs are made of one (or several) permanent magnet(s) and coil(s). The dynamic transduction processes they generate are produced by

electromagnetic fields from the different constituting elements through a lift-off usually assumed to be made of air. The mechanical sources are generated in a thin layer below the solid free (of coupling medium) surface. The layer thickness depends on both characteristics of the excitation fields involved and on the ability of the solid medium to transform them into dynamic mechanical energy. The operating principle of an EMAT is shown in figure 1:

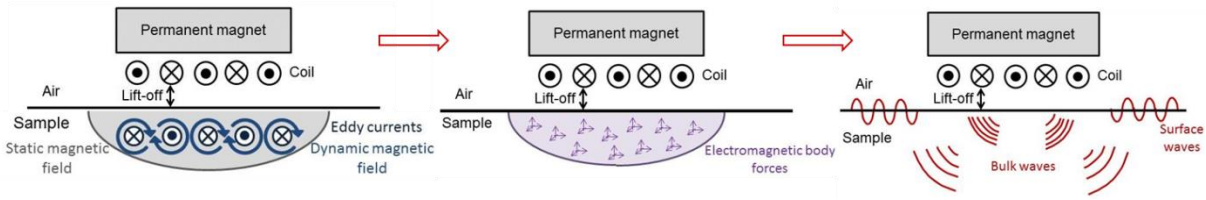

Figure 1. Operating principle of an ElectroMagnetic Acoustic Transducer (EMAT).

Three main electromagnetic dynamic excitations coexist in case of ultrasounds generation by EMAT into a ferromagnetic material. They are discussed in the following subsections.

1.1. Lorentz force

This fundamental phenomenon appears in any conductive material. It represents the force which acts on moving charges [4,5]. In EMAT applications, the magnetic Lorentz force stems from the interaction between the eddy currents density $\mathbf{J}$ $[\mathrm{A.m^{-2}}]$ and the magnetic induction field $\mathbf{B}$ [T] in the material, with a static component produced by the permanent magnet and a dynamic one generated by the coil. The Lorentz body force per unit volume $[\mathrm{N.m^{-3}}]$ is commonly expressed as:

$$\mathbf{f^L} = \mathbf{J} \times \mathbf{B}. \tag{1}$$

1.2. Magnetisation force

This dynamic excitation is specific to ferromagnetic materials and can be understood as the force acting on atomic magnetic moments inside the material in the presence of a spatially varying magnetic field. Indeed, ferromagnetic materials are divided up into magnetic domains, namely the Weiss domains separated by Bloch interfaces, within which the orientation of all the particle magnetic moments are aligned along the same direction [6]. The application of an external magnetic field on a ferromagnetic material reorganizes the orientation of these atomic magnetic moments in order to align them along the external magnetic field direction, as illustrated below in figure 2:

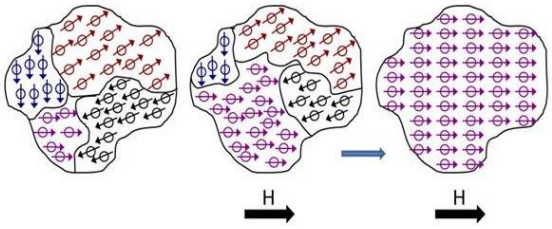

Figure 2. Weiss domains and atomic magnetic moment reorientation under external magnetisation.

The magnetisation process is then the force responsible for the reorientation of these atomic magnetic moments inside the sample, and corresponds finally to a macroscopic evidence of microscopic phenomena. The expression of the magnetisation body force per unit volume $[\mathrm{N.m^{-3}}]$ takes several forms in the literature which can lead to theoretical confusion, principally due to the choice of the magnetic fields involved in this phenomenon. It is not the purpose of this work to properly address the question of what formulation is the most appropriate. Denoting the magnetisation field by $\mathbf{M}$ $[\mathrm{A.m^{-1}}]$ and the magnetic field by $\mathbf{H}$ $[\mathrm{A.m^{-1}}]$, the expression of the magnetisation body force adopted here (taken from [4,5]) is given by the relation:

$$\mathbf{f^M} = \mu_0(\mathbf{M}.\boldsymbol{\nabla})\mathbf{H}, \tag{2}$$

where μ_0 [H. m^{-1}] is the magnetic permeability in vacuum.

1.3. Magnetostrictive effects

This phenomenon is also specific to ferromagnetic materials. It is related to magnetoelastic interactions at the material microscopic scale. Precisely, the 'magnetostriction' term stands for all the elastic variations of a magnetic material under external magnetic fields. Several types of magnetostrictive effects (direct or inverse) are referenced in the literature [5,6]. Here, the discussion is focused on the longitudinal Joule's magnetostriction, cited as the main impacting effects in our applications area [6,7]. These magnetostrictive effects result from the displacement of Bloch interfaces within the ferromagnetic part under external magnetisation, which creates a strain at the macroscopic scale measured along the magnetisation direction. Like the magnetisation force, the magnetostrictive effects depict a macroscopic manifestation of microscopic phenomena, which can be illustrated by figure 3:

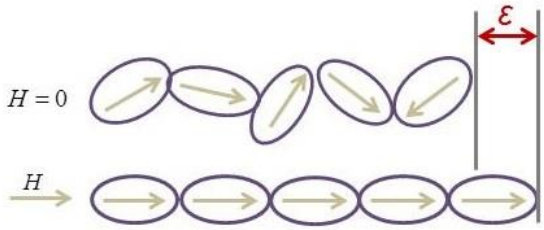

Figure 3. Magnetostrictive strain measured along the external magnetic field.

As mentioned, this phenomenon reduces at the macroscopic scale to a dimensional change (a strain). For the sake of an efficient semi-analytical model of ultrasound generation by EMAT, a model allowing the transformation of this magnetostrictive deformation into an equivalent body force of magnetostriction is needed. This is the purpose of the next section.

2. Modelling the equivalent body force of magnetostriction under a strong static magnetic field

The aim here is to establish an equivalent body force model which faithfully represents the direct longitudinal Joule's magnetostriction phenomenon previously described, that is to say, the macroscopic material deformation under an external magnetisation varying both with time and space. We assume first that these effects are magnetically isotropic at macroscopic scale and create isovolume dimensional change. These assumptions are commonly encountered in the literature [2,6,8], but an extension of the model could easily be done if needed to avoid making them. A weak magnetoelastic coupling is also assumed inside the ferromagnetic part. This could be justified by considering that the involved electromagnetic interaction volume is only restricted to a thin surface layer of the material which is limited by the electromagnetic skin depth:

$$\delta = \sqrt{\frac{1}{\pi f \mu \sigma}}, \tag{3}$$

where f is the inspection frequency, μ is the magnetic permeability, and σ the electric conductivity of the material being tested. Since the electromagnetic skin depth δ is much smaller than the wavelength λ of the acoustic wave produced in most EMAT applications ($\delta \ll \lambda$), the elastic waves which propagate below the surface into the part are assumed not to appreciably alter the electromagnetic fields confined in this close electromagnetic interaction vicinity of the part surface.

Under such assumptions, the electromagnetic quantities are known by solving the classical set of Maxwell's equations inside the concerned material volume (in a quasi-static approximation considering the inspection frequencies generally below than 10 MHz in our application cases). The

problematic addressed here is then to rigorously formulate the magnetostrictive transduction process starting from the knowledge of these electromagnetic fields. Inspired by [9], the idea in the present work is to model the three-dimensional magnetostrictive strain ε_{ij}^{MS} from the magnetic field $\mathbf{H}$ as:

$$\varepsilon_{ij}^{MS}(\mathbf{H}) = \lambda(\|\mathbf{H}\|)S_{ij}(\mathbf{H}). \quad (4)$$

This tensorial formulation involves two main terms which respect all the assumptions being made:

- The elementary magnetostrictive strain λ is measured in the direction of magnetisation and is only dependent on the studied material and the magnetic field intensity $\|\mathbf{H}\|$. This parameter is assumed to be a scalar in order to fulfil the macroscopic magnetic isotropy hypothesis, and can be obtained for example by interpolation of experimental data, as illustrated in figure 4:

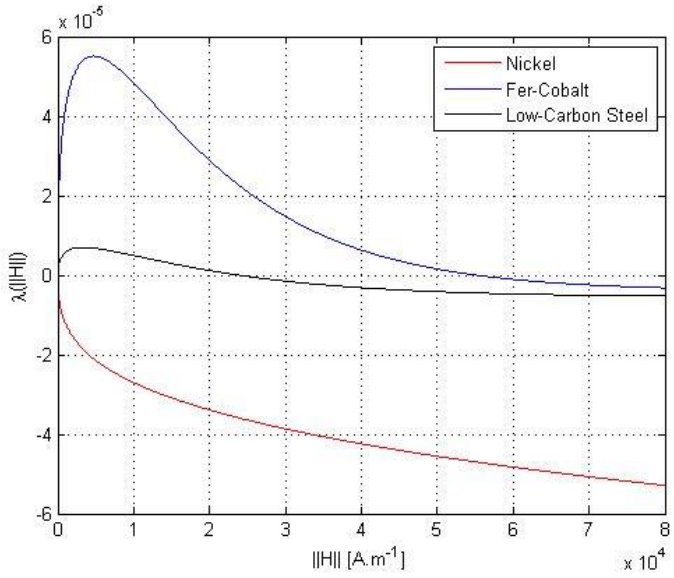

Figure 4. Dependency of the elementary magnetostrictive strain with the magnetic field intensity.

The formulation can also be easily extended to the case of magnetically anisotropic materials by considering $\boldsymbol{\lambda}$ as a second order tensor, written for example in the basis of easy magnetisation axes [6,10].

- The magnetic direction tensor $\mathbf{S}$ is a second order symmetric tensor only depending on the direction of the total magnetic field $\mathbf{H}$, and is expressed as:

$$\mathbf{S}(\mathbf{H}) = \frac{1}{2\|\mathbf{H}\|^2}(3\mathbf{H}\otimes\mathbf{H} - \|\mathbf{H}\|^2\mathbf{I}), \quad (5)$$

where the symbol $\otimes$ denotes the tensor product and $\mathbf{I}$ is the second order identity tensor. The tensor $\mathbf{S}$ is defined irrespective of the coordinate system used and helps modelling an isovolume dimensional change by verifying a null trace. It formulates this assumption by catching the principal direction of the total magnetic field and by assigning half the opposite value in the two other perpendicular directions. For example, in case of a total magnetic field $\mathbf{H} = H_3\mathbf{e_3}$, this tensor takes the following form:

$$\mathbf{S} = \begin{pmatrix} -0.5 & 0 & 0 \\ 0 & -0.5 & 0 \\ 0 & 0 & 1 \end{pmatrix}. \quad (6)$$

Based on this representation of the magnetostrictive strain, the next fundamental mathematical step relies on the fact that the total magnetic field is a superposition of a static part (induced by the

permanent magnet(s)) and of a dynamic part (induced by the coil(s)). In most EMAT applications, the intensity of the current flowing in the coil is small enough to ensure that the dynamic part of the magnetic field is much smaller than the static bias magnetic field. So, one has:

$$\mathbf{H} = \mathbf{H_S} + \mathbf{H_D}, \text{ with: } \mathbf{H_D} \ll \mathbf{H_S}. \tag{7}$$

Considering the magnetostrictive strain ε_{ij}^{MS} as a function of the magnetic field $\mathbf{H}$, its first order Taylor expansion around the static magnetic field $\mathbf{H_S}$ position leads to:

$$\varepsilon_{ij}^{MS}(\mathbf{H} = \mathbf{H_S} + \mathbf{H_D}) = \varepsilon_{ij}^{MS}(\mathbf{H_S}) + \frac{\partial \varepsilon_{ij}^{MS}}{\partial H_k}(\mathbf{H_S}) H_{Dk} + o(\|\mathbf{H_D}\|^2). \tag{8}$$

This simple development is particularly suitable since it provides a rigorous mathematical formulation which enables a relevant physical interpretation of the magnetostrictive phenomenon under the assumption of a strong static magnetic field. Indeed, the first term $\varepsilon_{ij}^{MS}(\mathbf{H_S}) = \lambda(\|\mathbf{H_S}\|) S_{ij}(\mathbf{H_S})$ depicts the time-independent longitudinal magnetostrictive strain which appears along the static field, and which can be seen as a spontaneous initial state of the ferromagnetic material under the external static magnetic field. The second term is the time-dependent leading term which gives rise to the ultrasonic elastic waves into the sample. It involves the third order piezomagnetic strain tensor d_{ijk}^{MS} evaluated at the static magnetic position and defined by the partial derivative of the magnetostrictive strain over the total magnetic field. This tensor is widely used in the literature when dealing with the linearized magnetoelastic coupled equations (see for example [2,11]). Taking benefits from the analytical tensorial expression of $\mathbf{S}$, one can derive an analytical expression for the piezomagnetic strain tensor d_{ijk}^{MS} by means of some tensorial and differential analyses:

$$\mathbf{d^{MS}}(\mathbf{H}) = \frac{\partial \boldsymbol{\varepsilon}^{\mathbf{MS}}}{\partial \mathbf{H}} = \frac{\varphi(\|\mathbf{H}\|)}{\|\mathbf{H}\|} \mathbf{S} \otimes \mathbf{H} + \frac{3\lambda(\|\mathbf{H}\|)}{\|\mathbf{H}\|^2} \left[\frac{\mathbf{H} \underline{\overline{\otimes}} \mathbf{I}}{2} - \frac{\mathbf{H} \otimes \mathbf{H} \otimes \mathbf{H}}{\|\mathbf{H}\|^2} \right], \text{with: } \varphi(\|\mathbf{H}\|) = \lambda'(\|\mathbf{H}\|). \tag{9}$$

In the previous expression, the operator $\underline{\overline{\otimes}}$ between a vector $\mathbf{v}$ and a second order tensor $\mathbf{T}$ is given in Voigt notation by: $\left[\mathbf{v} \underline{\overline{\otimes}} \mathbf{T}\right]_{ijk} = v_i T_{jk} + v_j T_{ik}$. This analytical tensorial expression is interesting since it models a general way to study the dynamic component of the magnetostrictive strain irrespective of the EMAT configuration and the geometry of the ferromagnetic part, which is quite missing in the literature. By using the elastic stiffness tensor $\mathbb{C}$, the piezomagnetic stresses can be written as:

$$\boldsymbol{\sigma}^{\mathbf{MS}} = -\mathbb{C} : \left[\boldsymbol{\varepsilon}^{\mathbf{MS}}(\mathbf{H_S}) + \mathbf{d^{MS}}(\mathbf{H_S}).\mathbf{H_D} \right], \tag{10}$$

where the symbol : denotes the tensorial double contraction product. This expression must be completed by taking into account free surface boundary condition in order to reproduce the physical context of the study (for example discussed in [1]). Denoting by $\partial\Omega$ the part surface and by $\mathbf{n}$ the outgoing normal vector to $\partial\Omega$, this condition is given by:

$$\boldsymbol{\sigma}^{\mathbf{MS}}.\mathbf{n} = \mathbf{0} \quad \text{on } \partial\Omega. \tag{11}$$

Finally, by taking the divergence of these piezomagnetic stresses, the modelling of equivalent body force of magnetostriction is achieved:

$$\mathbf{f^{MS}} = \boldsymbol{\nabla}.\boldsymbol{\sigma}^{\mathbf{MS}}. \tag{12}$$

The useful aspect of the mathematical approach in the present paper comes from its ability to deal with arbitrary coordinate system, allowing us to derive such a magnetostrictive equivalent body force for ferromagnetic parts of complex shape and irrespective of EMAT configuration. Of course, literature results for simpler cases can be straightforwardly derived from this model. For example,

when an elastic homogeneous isotropic planar material in the x-y plane is considered with a static magnetic field along the depth of the material ($\mathbf{H_S} = \mathrm{H_S}\mathbf{e_z}$), the formulation presented here reduces to the academic expression of the magnetostrictive body force given by [1,2]:

$$\mathbf{f^{MS}} = \begin{pmatrix} \mu_L \varphi(\mathrm{H_S}) \frac{\partial \mathrm{H_{Dz}}}{\partial x} - \frac{3\mu_L \lambda(\mathrm{H_S})}{\mathrm{H_S}} \frac{\partial \mathrm{H_{Dx}}}{\partial z} \\ \mu_L \varphi(\mathrm{H_S}) \frac{\partial \mathrm{H_{Dz}}}{\partial y} - \frac{3\mu_L \lambda(\mathrm{H_S})}{\mathrm{H_S}} \frac{\partial \mathrm{H_{Dy}}}{\partial z} \\ -2\mu_L \varphi(\mathrm{H_S}) \frac{\partial \mathrm{H_{Dz}}}{\partial z} - \frac{3\mu_L \lambda(\mathrm{H_S})}{\mathrm{H_S}} \left[\frac{\partial \mathrm{H_{Dx}}}{\partial x} + \frac{\partial \mathrm{H_{Dy}}}{\partial y}\right] \end{pmatrix}, \quad (13)$$

where μ_L is the second Lamé's parameter (shear modulus).

By using the presented model of magnetostrictive equivalent body forces, the next section aims at giving a suitable mathematical process enabling to accurately and efficiently predict the ultrasonic field radiated by the dynamic magnetostrictive sources generated by EMAT.

3. Transformation into magnetostrictive equivalent surface stresses

3.1. General concept of mathematical transformation of body forces into equivalent surface stresses

In ultrasonic nondestructive evaluation (NDE), accurate knowledge of the ultrasonic field radiated by the source is of paramount importance as soon as quantitative results are expected, that is to say, if the method of examination is designed to go as far as defect characterization and sizing. For this reason, in the vast literature, many models have been developed to compute field radiation by ultrasonic sources. Among them, many models were developed to predict fields radiated by mechanical sources operating at the surface of the solid, as those generated by piezoelectric transducers in direct contact. The calculation of the elastic wave field radiated by a point-source of normal or tangential stress in an elastic half-space, that is to say, the Green's function of the so-called Lamb's problem, is the subject of hundreds of papers in the literature, including exact, approximate or numerical solutions and dealing with a variety of elastic media, after Lamb's pioneering contribution [12]. For finite-size sources, a simple surface and time convolution of the time-dependent surface stress distribution with one such solution for a point source leads to predict source diffraction effects [13]. It is our aim to use this kind of time and surface convolution models to predict the field radiated by non-contact sources. But since at this stage, all the dynamic excitations induced by EMAT in ferromagnetic materials are expressed as a volume distribution of electromagnetic body forces, a mathematical method is needed to accurately transform these body forces into equivalent surface stresses distribution, that is to say, which radiate the same ultrasonic field into the mechanical part.

Let us consider an open set Ω embodying the elastic domain of the part under test. We want to study the representation of particle displacement field $\mathbf{u}(\mathbf{x})$ radiated at an observation point $\mathbf{x} \in \Omega$ by a distribution of time-harmonic body force $\mathbf{f}(\mathbf{x_0})e^{i\omega t}$, where ω denotes the angular frequency and $\mathbf{x_0} \in \Omega$ denotes the source points. For clarity, the factor $e^{i\omega t}$ will be omitted in what follows. The exact way for determining the particle displacement field consists in a spatial volume convolution integral of body forces $\mathbf{f}(\mathbf{x_0})$ with the Green's tensor $\mathbf{G}(\mathbf{x}, \mathbf{x_0})$ for elastic waves in Ω. So the idea of this section is to determine the most accurate surface distribution of equivalent stresses $\tilde{\boldsymbol{\sigma}}^{\mathbf{f}}$ of the body force $\mathbf{f}$, which approximates the most faithfully the particle displacement $\mathbf{u}$ by a surface convolution with the same previous Green's tensor taken at the part surface. The approach is summed up by the relation:

$$\mathbf{u}(\mathbf{x}) = \iiint_{\mathbf{x_0} \in \Omega} \mathbf{G}(\mathbf{x}, \mathbf{x_0}).\mathbf{f}(\mathbf{x_0}) d\Omega \approx \iint_{\mathbf{X_0} \in \partial\Omega} \mathbf{G}(\mathbf{x}, \mathbf{X_0}).\tilde{\boldsymbol{\sigma}}^{\mathbf{f}}(\mathbf{X_0}) d\Gamma. \quad (14)$$

The usual method for deriving equivalent surface stresses consists in a simple integration of the body forces over the depth (depicted by a variable w), which corresponds to the zeroth order force moment:

$$\tilde{\boldsymbol{\sigma}}^{\mathbf{f}} = \mathbf{M}_{\mathbf{f}}^{(0)} = \int_w \mathbf{f}(\mathbf{x_0}) \mathrm{K}(w) dw, \quad (15)$$

where K(w) denotes the local curvatures at a depth w of the part surface. But Thompson [14] pointed out in an ideal academic case (illustrated below in subsection 3.2.) that such a simple integration over the material depth predicts wrong stresses in case of magnetostrictive effects, mostly due to the free surface boundary condition previously discussed. This is the reason why Thompson [15], and more recently Rouge *et al.* [16], proposed a new model of equivalent surface stresses in elastic isotropic planar cases. It relies on a second order Taylor expansion in the direction normal to the part surface of the Green's integral formulation of the elastic wave equation and takes into account the moments of a body force distribution up to the second order, the p-th order force moment being denoted by $\mathbf{M_f^{(p)}}$. In order to make this mathematical transformation applicable even broadly and so, consistently with the general magnetostrictive body force model presented in section 2, this approach has been recently extended to surfaces of complex shape and anisotropic elastic materials by means of tensorial and differential analyses [17]. The model takes into account the angular inspection frequency ω, the mass density ρ, the elastic stiffness tensor $\mathbb{C}$, the outgoing normal vector to the studied surface $\mathbf{n}$, and can be reduced for the sake of clarity to the relation:

$$\tilde{\boldsymbol{\sigma}}^{\mathbf{f}} = \tilde{\boldsymbol{\sigma}}^{\mathbf{f}}\left(\mathbf{M_f^{(p)}}, \omega^2, \rho, \mathbb{C}, \mathbf{n}\right), \quad p = 0,\ 1,\ 2. \tag{16}$$

Readers are referred to [17] for the detailed expression of this transformation. This mathematical model has also been numerically validated on bi-dimensional cases in order to demonstrate its accuracy gained in the particle displacement representation by a surface convolution. To maintain the process generality, this transformation method has been derived irrespective of nature of body forces considered. The only hypothesis is that these body forces satisfy a penetration depth much smaller than the acoustic wavelength λ, which is of course verified in EMAT applications considering that $\delta \ll \lambda$. The following subsections give 2D and 3D implementation examples of the magnetostrictive equivalent surface stresses distributions computed both by the usual method of simple integration (referenced as 'Order 0 method') and by the presented transformation model (referenced as 'Order 2 method').

3.2. *2D application example of the model in ideal EMAT configuration*

We present here the ideal and analytical 2D case historically studied by Thompson [14], which gave him the idea of a model based on a second order expansion of the equivalent surface stresses. It consists of a meander line coil carrying a current $Ie^{i\omega t}$ at the desired ultrasonic frequency ω and positioned below a permanent magnet delivering a static uniform magnetic field $\mathbf{H_S} = H_S\mathbf{e_x}$. Dynamic eddy currents and magnetic fields are set up at the surface of the ferromagnetic material (of relative magnetic permeability μ_R). Besides the uniform character of the static field, this case is ideal because it further assumes an infinite y extent and a dynamic magnetic field $\mathbf{H_D}$ only along the x direction (parallel to the static magnetic field). The EMAT configuration under study is illustrated in figure 5:

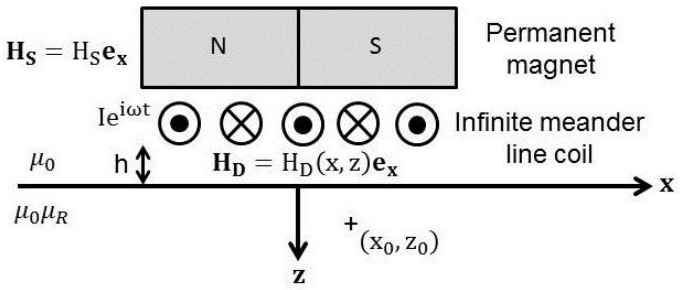

Figure 5. Thompson's 2D EMAT configuration.

As shown by Thompson [15], when this transducer has an infinite y extent and both static and dynamic fields in the x direction, it produces a force distribution on a ferromagnetic material with a component in the z-direction of the form:

$$f_z^{MS}(x_0, z_0) = \mu_L \varphi(H_S)[ik - \delta_D(z_0)]H_{Dx}(x_0)e^{-ikz_0}e^{i\omega t}, \quad (17)$$

where $k = (1 - i)/\delta$, (x_0, z_0) are the coordinates of a source point below the surface, and δ_D denotes a Dirac delta function at the part surface. In this ideal planar 2D case, it is worth noting that the model of equivalent magnetostrictive body force presented in section 2 reduces well to the magnetostrictive force given by Thompson, excepted for the Dirac delta function term. Indeed, this term is of non-physical nature and only artificially added at the end of the force derivation process by Thompson in order to satisfy the otherwise violated stress-free boundary condition. As mentioned above, the model presented here also takes into account a free surface boundary condition, but in the very definition of the piezomagnetic stresses, and so, without adding any non-physical term in the magnetostrictive force definition. Then, the zeroth and second order moments of the magnetostrictive normal body force can be calculated as follows:

$$M_{MSz}^{(0)}(x_0) = \int_{z_0=0}^{+\infty} f_z^{MS}(x_0, z_0)dz_0 = 0 \quad (18a)$$

$$M_{MSz}^{(2)}(x_0) = \int_{z_0=0}^{+\infty} z_0^2 f_z^{MS}(x_0, z_0)dz_0 = -\frac{2\mu_L \varphi(H_S)}{k^2} H_{Dx}(x_0)e^{i\omega t} \quad (18b)$$

Therefore, while the zeroth order moment of the magnetostrictive normal force vanishes, its second order moment is finite and non-zero. Thompson [15] made two independent observations to explain the inconsistency of predicting null surface stresses of magnetostriction in this case, which inspired him the idea of developing the equivalent surface stresses model up to a second order. The model was historically only designed for an elastic isotropic planar half-space, which has been corrected by Rouge *et al.* [16], and recently extended to media of complex shape and numerically validated [17]. In this special analytic configuration, the whole second order expansion of equivalent surface stresses model reduces to:

$$\tilde{\sigma}_z^{f^{MS}}(x_0) = M_{MSz}^{(0)}(x_0) - \frac{\rho\omega^2}{2(\lambda_L + 2\mu_L)} M_{MSz}^{(2)}(x_0) = \frac{\rho\omega^2 \mu_L \varphi(H_S)}{(\lambda_L + 2\mu_L)k^2} H_{Dx}(x_0)e^{i\omega t} \quad (19)$$

Besides the reasons given by Thompson in [15], this result has also been confirmed in [11] by considering the magnetostrictive interaction with ferromagnetic part as a pure inertial phenomenon, result that was numerically validated using finite-elements method. So, even if these equivalent surface stresses (being proportional to the ratio δ^2/λ^2) are weak in this ideal case, this study gives credit to the whole methodology since the equivalent surface stresses prediction by a second order expansion is non-zero. Moreover, the main advantages of the two mathematical models presented here (meaning the equivalent magnetostrictive body force and its equivalent surface stresses expanded to a second order) rely on their ability to be applicable in three-dimensional 'non-ideal' cases (that is to say without considering any infinite dimension extent) and irrespective of the EMAT configuration. The models allow therefore studying the surface variations of the electromagnetic fields produced by more complex configurations of EMAT with finite-size aperture over the excited surface. Results of such three-dimensional computations are given in the following subsection.

3.3. 3D computations of the equivalent surface stresses of magnetostriction

As mentioned above, we show here some computation results for three-dimensional configurations of EMAT with a finite-size aperture over the excited surface of a ferromagnetic material. Results in this subsection - meaning the computation of the EMAT configuration, the definition of the material elastic and electromagnetic properties, the calculation of the electromagnetic fields induced, the magnetostrictive body force and finally its equivalent surface stresses - were obtained by

implementing the mathematical models presented in sections 2 and 3 in the Eddy Current Testing (ECT) modulus of the CIVA software platform [18] developed at CEA List and dedicated to simulation of various non-destructive evaluation techniques.

The assumptions made on the magnetic behaviour of the tested material need to be clearly described here. We first assume that the material does not exhibit an intrinsic permanent magnetisation; the magnetisation is thus purely induced by the magnetic excitation field. The constitutive relations of the ferromagnetic material are given by:

$$\mathbf{M} = \boldsymbol{\chi}(\mathbf{H}) \,.\, \mathbf{H} \quad \text{and} \quad \mathbf{B} = \mu_0(\mathbf{H} + \mathbf{M}) = \boldsymbol{\mu}(\mathbf{H}) \,.\, \mathbf{H},$$

where $\boldsymbol{\chi}$ is the material magnetic susceptibility, and $\boldsymbol{\mu} = \mu_0(\mathbf{1} + \boldsymbol{\chi}) = \mu_0 \boldsymbol{\mu}_\mathbf{R}$ is the material magnetic permeability. Numerous theoretical models and experimental analyses are devoted to characterize these two key magnetic parameters, taking into account magnetic anisotropy, non-linear hysteretic behaviour, their dependencies on frequency, on temperature, or on applied stress. In order to make simpler our analysis on magnetostrictive effects, anhysteretic behaviour and magnetic isotropy are assumed in the present work and μ is modelled by a constant scalar parameter. This ideal case does not faithfully represent all possible experimental cases of magnetic behaviour; hysteretic behaviour and the dependency on frequency or on applied stress have a potential impact on the ultrasound generation processes involved in EMAT applications. Nevertheless, since a frequency domain simulation is performed with a weak coil injection current (below 1A) which presents a simple sinusoidal dependency with a frequency below 10 MHz, such assumptions constitute a good starting approximation to model soft ferromagnetic material behaviour focusing on the magnetostrictive model presented here.

The simulation case under study in the present paper is a 3D EMAT composed of a cubic permanent magnet with an induction intensity of 1 T positioned over a rectangular spiral coil with an excitation current intensity of 1 mA at an excitation frequency $f = 5$ MHz. The studied ferromagnetic material is a planar low-carbon steel with a relative magnetic permeability $\mu_R = 2$ and an electric conductivity $\sigma = 2\ \mathrm{MS.m^{-1}}$. It is further assumed elastically isotropic with the elastic quantities: $\rho = 7.8\ \mathrm{g.cm^{-3}}$, $c_P = 5900\ \mathrm{m.s^{-1}}$, and $c_S = 3230\ \mathrm{m.s^{-1}}$. The lift-off (in air) distance between the coil and the material is fixed at 0.2mm. An illustration of the studied EMAT configuration is given in figure 6:

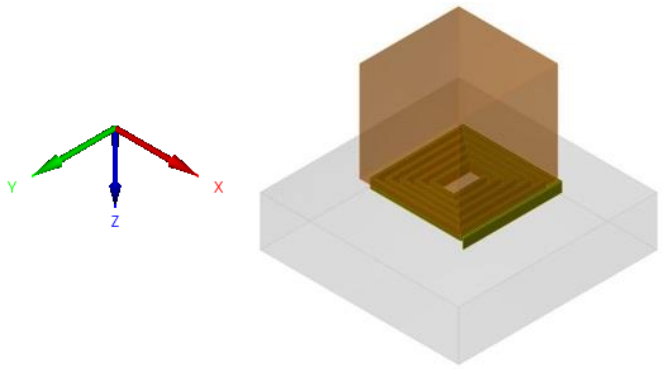

Figure 6. 3D EMAT composed of a cubic permanent magnet and a rectangular spiral coil.

Figure 7 displays the numerical simulation results using either a zeroth or a second order expansion of the equivalent surface stresses of the magnetostrictive equivalent body force induced by the EMAT in the detailed configuration, with a static magnetic induction $\mathbf{B_S}$ respectively along the x-direction (top) and along the z-direction (bottom).

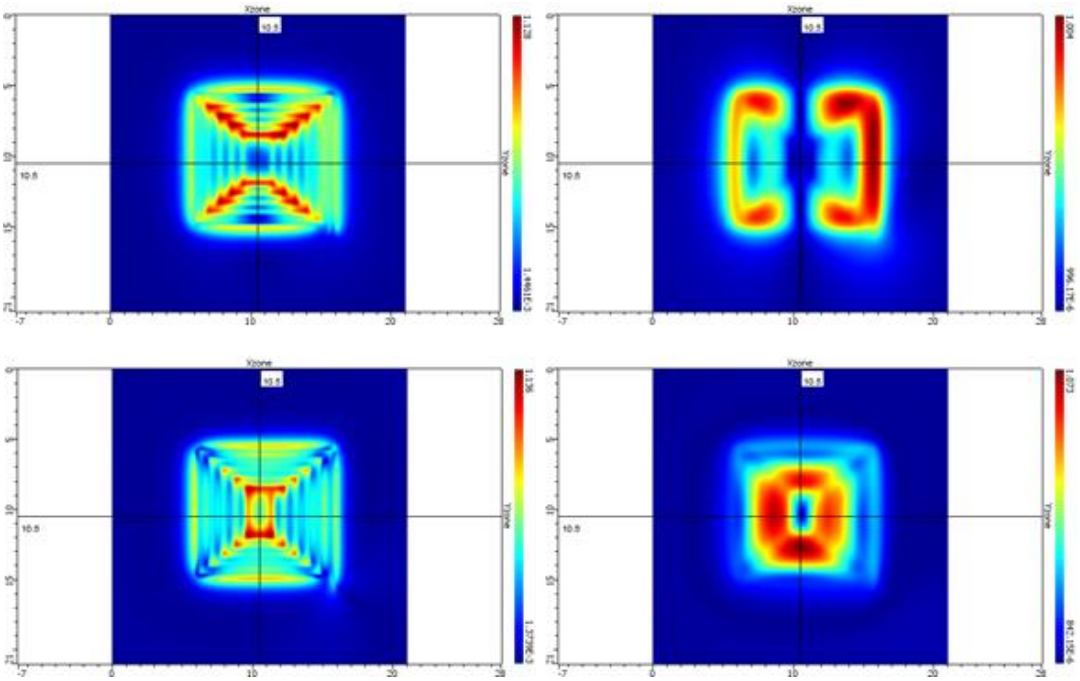

Figure 7. Norm of magnetostrictive equivalent surface stresses. Left: Order 0; Right: Order 2. Top: $\mathbf{B_S}$ along x. Bottom: $\mathbf{B_S}$ along z.

As we can observe on the norm of the equivalent surface stresses of magnetostriction, the zeroth order expansion (meaning the zeroth order force moment) of equivalent surface stresses does not vanish anymore as in the above 2D case, since the x and y components of the electromagnetic fields and of the surface stresses coexist. We can conclude from these figures that the magnetostrictive phenomenon is much more precisely predicted using a second order expansion model of equivalent surface stresses, since the results between the two models are quite radically different. An explanation can be found in [11] in considering the magnetostriction phenomenon as a pure inertial force. In fact, the second order expansion model of the equivalent surface stresses accounts for the inertial effects brought by the elastic wave equation; this is actually why the model is sensitive to the square of the angular frequency ω^2. The discussion confirms that magnetostriction effects are mostly due to inertial phenomenon, which can be modelled by the equivalent surface stress model detailed in section 3.

The next section uses these magnetostrictive equivalent surface stresses as source terms to predict the longitudinal (L) and transversal (T) elastic waves generated by this configuration of EMAT into the mechanical part being tested.

4. Simulation of the ultrasonic field radiated by magnetostrictive effects induced by EMAT

Finally, the modelling work done in the two previous sections allows taking benefits from well-established semi-analytical models of ultrasonic field radiation to predict the elastic wave field radiated by magnetostrictive effects induced by an EMAT into a ferromagnetic part. The setup here is the one described in the above section, using the detailed EMAT with a static magnetic induction $\mathbf{B_S}$ along the z-direction. Figures 8-9 depict respectively the longitudinal and transversal waves radiated into planar elastically isotropic low-carbon steel at a frequency $f = 5$ MHz. Results are given using either a zeroth or a second order expansion of the equivalent surface stresses of the magnetostrictive equivalent body force, and the relative differences ϵ_r (in percent) between the two transformation methods is represented according to the relation:

$$\epsilon_r = \left| \frac{u^{order2} - u^{order0}}{\max(u^{order2}, u^{order0})} \right|. \quad (20)$$

Maximum ultrasonic amplitude of the particle displacement modulus (in arbitrary units) radiated into the material is shown for a set of calculation points in a plane perpendicular to the piece surface (first row) and in a plane parallel to the surface at a depth of 50 mm (second row), for longitudinal waves (figure 8) and for transversal wave (figure 9).

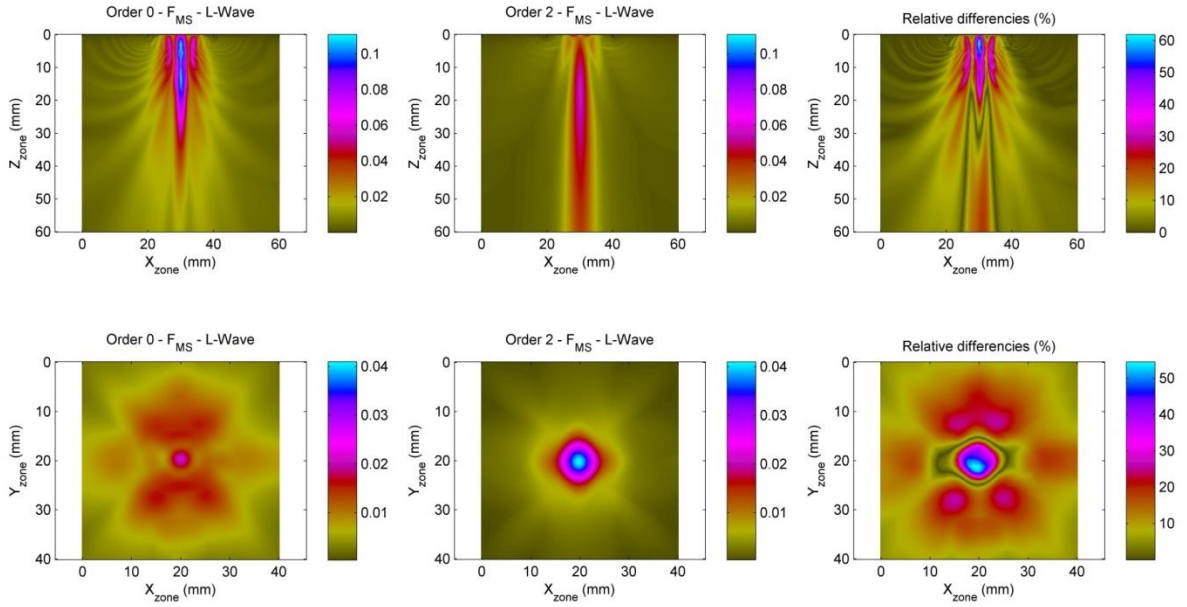

Figure 8. Map of the maximum L-wave amplitude induced by magnetostrictive effects. 1st row: in a plane *xz*, 2nd row; in a plane *xy* at a depth of 50 mm. 1st column: computed at the 0-th order, 2nd column: computed at the 2nd order, 3rd column: relative difference.

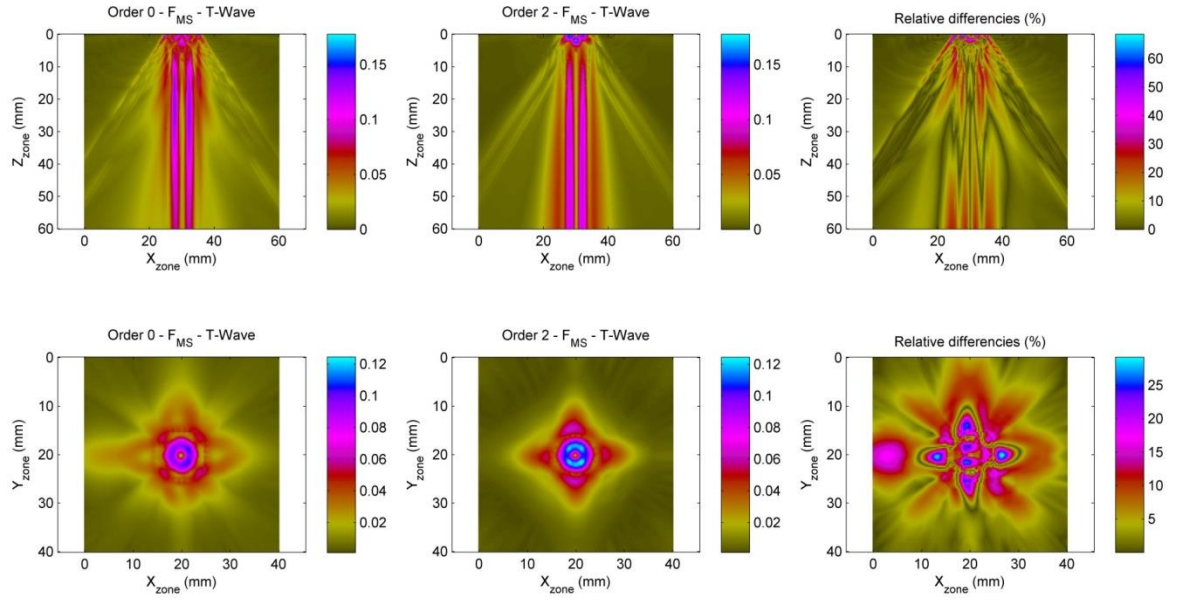

Figure 9. Same as figure 8, but T-wave radiation.

As expected in taking a look at the magnetostrictive equivalent surface stresses with either a zeroth or a second order expansion, ultrasonic fields radiated by these two transformation models are radically different, with a maximum relative error higher than 60 % at some observation points inside the low-carbon steel part.

It is also possible to numerically simulate all the transduction processes involved in the ultrasonic generation by an EMAT into a ferromagnetic part, that is to say, to simulate the Lorentz force, the magnetisation force and the magnetostriction effects. For example, figure 10 shows the fields at 50-mm-depth of transversal ultrasonic wave generated by the EMAT above-described with a static magnetic induction $\mathbf{B_S}$ along the x-direction with the body forces taken separately and all together:

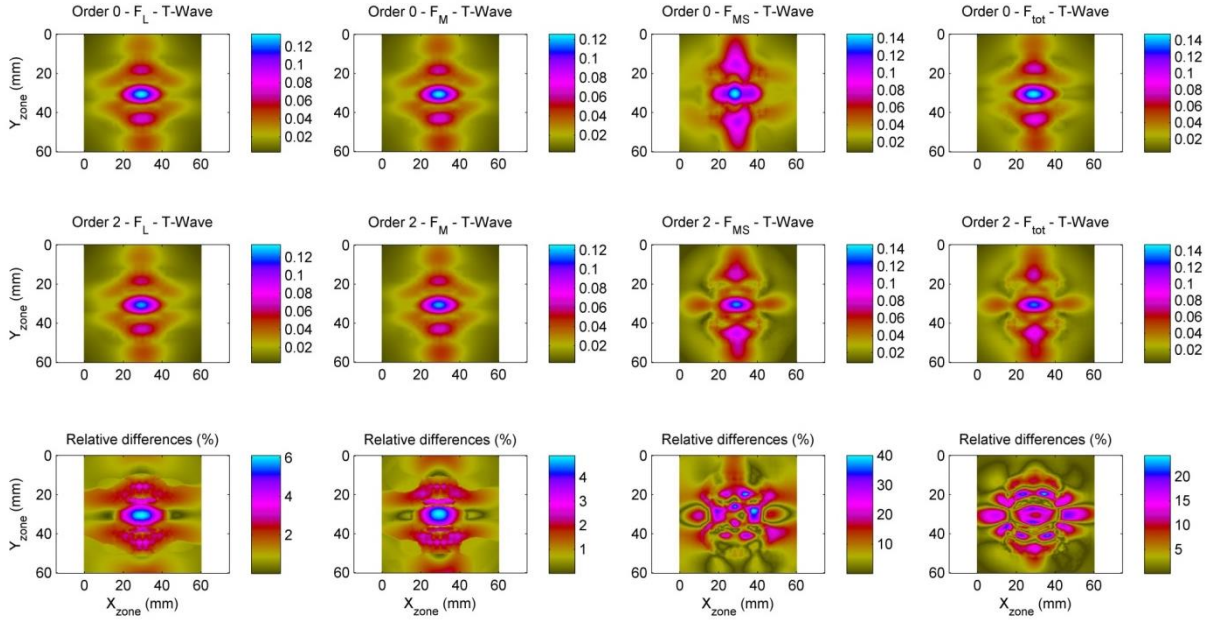

Figure 10. Maps of the maximum ultrasonic amplitude in a plane *xy* induced by all the EMAT source excitations. 1st row: 0-th order, 2nd row: 2nd order, 3rd row: relative difference. 1st column: Lorentz force, 2nd column: magnetisation force, 3rd column: magnetostriction effect, 4th column: total field.

As we can see, in this particular configuration, all the transduction processes induced by the EMAT play a role in the ultrasonic wave it generates, included the magnetostriction effects, as the amplitudes of the fields they radiate are of the same order of magnitude. In this particular configuration, it may also be observed that both the Lorentz and the magnetisation contributions look very much the same over the computation zone. Actually, they show very similar variations of the modulus of the amplitude in this zone, but their signs are opposite so that they interfere destructively. This result is well-known for a tangential static field (for example in [2]). As a consequence, the remaining field is essentially related to magnetostrictive effects; this is easily seen by comparing the maps corresponding to the field radiated by magnetostriction with those corresponding to the sum of all contributions.

5. Discussions and conclusions

The work presented herein provides a rigorous mathematical definition of an equivalent body force model for the magnetostrictive effects under a strong static magnetic field and a weak magnetoelastic coupling. This model relies on a tensorial formulation making it suitable to deal with arbitrary EMAT configuration and arbitrary geometry of the part. From the magnetostrictive equivalent body force, the derivation of the magnetostrictive equivalent surface stresses is obtained with accuracy by means of a second order expansion model, which has been numerically validated in a previous work [17]. Finally, these two mathematical models allow predicting the ultrasonic field radiated by magnetostrictive effects in ferromagnetic parts for general inspection cases in using well-established semi-analytical radiation models. Thus, all the source phenomena involved in three-dimensional configurations of EMAT and the ultrasonic field they radiate can be both efficiently and accurately predicted.

The prospects of this work consist in obtaining experimental validations of the magnetostriction model discussed here; in extending the model in the time domain in case of a strong dynamic magnetic field; and in investigating further the weak magnetoelastic coupling assumption.

References

[1] Thompson R B 1990 *Physical Acoustics* **19** 157–200
[2] Hirao M and Ogi H 2003 *EMATs for Science and Industry: Noncontacting Ultrasonic Measurements* (Boston: Kluwer Academic Publishers)
[3] Walaszek H and Bouteille P 2014 ECNDT proceedings published on-line, www.ndt.net/events/ECNDT2014/app/content/Paper/505_Walaszek.pdf
[4] Brown W F 1966 *Magnetoelastic Interactions* (Heidelberg: Springer-Verlag Berlin)
[5] Moon F C 1984 *Magneto-Solid Mechanics* (New York: John Wiley & Sons Inc)
[6] Bozorth R M 1964 *Ferromagnetism* (Hoboken: Wiley-Interscience)
[7] Lee E W 1955 *Rep. Prog. Phys.* **18** 184–229
[8] Chikazumi S 1964 *Physics of Magnetism* (New York: Wiley)
[9] Ebrahimi H, Gao Y, Kameari A, Dozono H and Muramatsu K 2013 *IEEE Trans. Magn.* **49** 1621–24
[10] Mason W 1954 *Phys. Rev.* **96** 302–10
[11] Ribichini R, Nagy P B and Ogi H 2012 *NDT &E* **51** 8–15
[12] Lamb H 1904 *Philos. Trans. R. Soc. Lond. Ser.* **A 203** 1–42
[13] Lhémery A 1994 *J. Acoust. Soc. Am.* **96** 3776–86
[14] Thompson R B 1978 *IEEE Trans. Sonics Ultrason.* **SU-25** 7–15
[15] Thompson R B 1980 *J. Nondestruct. Eval.* **1** 79–85
[16] Rouge C, Lhémery A and Ségur D 2013 *J. Acoust. Soc. Am.* **134** 2639–46
[17] Clausse B and Lhémery A 2016 *Wave Motion* **60** 135–48
[18] For detailed description of the platform, see www.extende.com